MOLECULAR AND CELLULAR BIOLOGY, Sept. 2005, p. 8251–8258 Vol. 25, No. 18
0270-7306/05/$08.00+0 doi:10.1128/MCB.25.18.8251–8258.2005
Copyright © 2005, American Society for Microbiology. All Rights Reserved.

Cell Cycle-Regulated Inactivation of Endothelial NO Synthase through NOSIP-Dependent Targeting to the Cytoskeleton

Michael Schleicher, Fredrik Brundin, Steffen Gross, Werner Müller-Esterl,* and Stefanie Oess

Institute for Biochemistry II, Cardiovascular Biochemistry, University of Frankfurt, Medical School, Theodor-Stern-Kai 7, 60590 Frankfurt, Germany

Received 10 February 2005/Returned for modification 7 April 2005/Accepted 21 June 2005

Nitric oxide (NO) plays a key role in vascular function, cell proliferation, and apoptosis. Proper subcellular localization of endothelial NO synthase (eNOS) is crucial for its activity; however, the role of eNOS trafficking for NO biosynthesis remains to be defined. Overexpression of NOS-interacting protein (NOSIP) induces translocation of eNOS from the plasma membrane to intracellular compartments, thereby impairing NO production. Here we report that endogenous NOSIP reduces the enzymatic capacity of eNOS, specifically in the G_2 phase of the cell cycle by targeting eNOS to the actin cytoskeleton. This regulation is critically dependent on the nucleocytoplasmic shuttling of NOSIP and its cytoplasmic accumulation in the G_2 phase. The predominant nuclear localization of NOSIP depends on a bipartite nuclear localization sequence (NLS) mediating interaction with importin α. Mutational destruction of the NLS abolishes nuclear import and interaction with importin α. Nuclear export is insensitive to leptomycin B and hence different from the CRM1-dependent default mechanism. Inhibition of NOSIP expression by RNA interference completely abolishes G_2-specific cytoskeletal association and inhibition of eNOS. These findings describe a novel cell cycle-dependent modulation of endogenous NO levels that are critical to the cell cycle-related actions of NO such as apoptosis or cell proliferation.

Endothelium-derived nitric oxide (NO) plays a key role in vascular function including angiogenesis, cell proliferation, and apoptosis (30). The short-lived character and the variety of biological targets of NO urge for tight temporal and spatial control of NO biosynthesis, reflected in the complex machinery modulating endothelial nitric oxide synthase (eNOS) activity (14). While the mechanisms of direct eNOS activation are quite well understood, the subcellular targeting of eNOS and its implication for NO bioavailability are subject to controversial discussions. Conventional wisdom holds that eNOS becomes activated at the plasma membrane, e.g., in response to vascular endothelial growth factor or shear stress (14, 30). It has been suggested, but is not generally accepted, that upon activation eNOS dissociates from the plasma membrane and translocates to the cytosol (14). Besides the plasma membrane, the Golgi complex represents a major target site for eNOS; however, it is unclear whether it also contains active eNOS, either as a consequence of activation in situ or due to the translocation of activated eNOS from plasma membrane to the Golgi (15). Circumstantial experimental evidence indicates that eNOS may also be targeted to the cytoskeleton and to intercellular junctions; however, the implications of these localizations for eNOS activity are also unclear. The detergent-insoluble pool, commonly considered to represent the cytoskeleton, has been claimed to be an "inactive" compartment for eNOS (18, 30). In contrast, eNOS has been reported to translocate to intercellular junctions and to associate with the actin cytoskeleton in response to cell-cell contact formation, concomitant with an increase in eNOS activity (13). Moreover, direct interaction of eNOS with actin has been demonstrated by coimmunoprecipitation studies, and the polymerization state of actin has been implicated in contributing to eNOS activity control (33).

We have hypothesized that intracellular trafficking of eNOS is a regulated process in which interacting proteins play crucial roles. Based on this hypothesis, we have recently identified two novel proteins that interact with eNOS, i.e., NOS-interacting protein (NOSIP) (6) and eNOS traffic inducer (NOSTRIN) (40), both of which interfere with eNOS plasma membrane association and NO production. Overexpression of NOSIP results in a displacement of eNOS from the plasma membrane to intracellular, Triton-insoluble compartments, accompanied by a significant reduction of NO release (6). Studies on the in vivo distribution of NOSIP and eNOS revealed a widespread cooccurrence of the two proteins in a variety of cell types (20). In the same study, we observed that NOSIP exhibits two distinct subcellular localization patterns showing either predominantly cytoplasmic or nuclear immunoreactivity (8, 20). The distribution pattern seems not to be determined by the cell type, since cytoplasmic and nuclear localization coexist, e.g., in hepatocytes (20). In this present study we aimed to characterize the molecular mechanisms underlying subcellular trafficking of NOSIP and the consequences for eNOS distribution and function.

MATERIALS AND METHODS

Constructs. Human NOSIP cDNA and mutants were cloned into pcDNA3.1 (Invitrogen), coding for an N-terminal myc tag. Enhanced green fluorescent protein (EGFP) fusion proteins were expressed from pEGFP-N1. cDNAs for human importin α (pGEX-4T-3; Amersham) and importin β (pGEX-6P-1; Amersham), coding for an N-terminal glutathione transferase (GST) fusion, were obtained from G. Blobel (HHMI, The Rockefeller University, New York, NY).

* Corresponding author. Mailing address: Institute for Biochemistry II, University of Frankfurt Medical School, Theodor-Stern-Kai 7, 60590 Frankfurt/Main, Germany. Phone: 49 69 6301 5652. Fax: 49 69 6301 5577. E-mail: wme@biochem2.de.

For NOSIP RNA interference (RNAi) CHO-NOS cells were transfected with a pTER$^+$ vector (37) containing the target sequence for knockdown of murine NOSIP (base pairs 758 to 777). As a control, target sequences specific for EGFP were used and referred to as unrelated RNAi.

Antibodies. Rabbit antisera AS600 and AS531 (6) raised against human NOSIP were used for NOSIP detection in CHO-NOS and HeLa cells, respectively. Antibodies directed against myc tag (9E10; Santa Cruz) eNOS, Nup62 (BD Transduction), glyceraldehyde-3-phosphate dehydrogenase (GAPDH; Abcam), and actin (Sigma Biochemicals) were used as indicated.

Cell culture and cell cycle blockage. HeLa cells and NIH 3T3 fibroblasts were maintained in Dulbecco's modified Eagle's medium (DMEM) containing 10% fetal calf serum and 1% penicillin-streptomycin. EA.hy926 cell medium was supplemented with hypoxanthine-aminopterin-thymidine. CHO cells stably expressing eNOS (CHO-NOS) were maintained as previously described (6). HeLa and CHO-NOS cells were transfected using Polyfect or Effectene (QIAGEN). HeLa and EA.hy926 cells were synchronized into G_1 phase by double thymidine block as previously described (28). CHO-NOS cells were blocked into G_1 by incubation with 1.5 mM hydroxyurea for 14 h and entered G_2 phase 6 h after block release. Dividing cells were removed by mitotic shake-off. For fluorescence-activated cell sorting (FACS) analysis, cells were washed with phosphate-buffered saline (PBS) and fixed in 70% ethanol overnight at 4°C. Cells were stained at 37°C for 30 min in 1 ml of PBS containing 10 μg/ml propidium iodide and 10 μg/ml RNase A. Cells were analyzed on a FACSCalibur cell analyzer using CellQuest software (Beckton Dickinson), and the cell cycle stages were determined using Cylchred software.

Indirect immunofluorescence. Cells seeded on coverslips were fixed and permeabilized with ice-cold methanol and blocked with PBS containing 0.1% Tween 20 (PBST) and 5% bovine serum albumin. Afterwards cells were incubated with primary antibodies (1:100), followed by incubation with Cy2- or Cy3-coupled secondary antibodies (1:500) and 4′,6′-diamidino-2-phenylindole (DAPI; 1 μg/ml). Images were acquired using a Zeiss Axiovert 200 in combination with Improvision Openlab software.

Western blotting. Protein samples were dissolved in sample buffer (200 mM Tris-HCl, pH 6.8, 6% sodium dodecyl sulfate [SDS], 20% glycerol, 10% dithiothreitol, 0.1 mg/ml bromophenol blue), separated by SDS-polyacrylamide gel electrophoresis and transferred to polyvinylidene difluoride membranes. The membranes were blocked in PBST containing 5% nonfat dry milk. Detection was carried out with primary antibody as indicated, in combination with horseradish peroxidase-conjugated antibody to rabbit or mouse immunoglobulin G, respectively, and the ECL detection system (Amersham).

Subcellular fractionation and detergent extraction. To obtain nuclear and cytoplasmic fractions, cells were washed and sampled in 500 μl of cold PBS. Pelleted cells (500 × *g*) were resuspended in hypotonic buffer (10 mM Tris-HCl, pH 7.4, 10 mM sodium iodide, 5 mM $MgCl_2$, 1 mM Pefabloc) and homogenized with 20 strokes in a tissue grinder. The supernatant (600 × *g*) was designated the cytoplasmic fraction. The pellet, representing the nuclear fraction, was washed with hypotonic buffer containing 0.1% NP-40 (Calbiochem). To obtain Triton-insoluble fractions, after optional pretreatment with cytochalasin D (1 μM), cells were washed and lysed in Triton buffer (1% Triton X-100, 20 mM Tris-HCl, pH 8.0, 137 mM NaCl, 2 mM EDTA, 1 mM Pefabloc) for 15 min on ice or at room temperature as indicated and centrifuged for 30 min at 15.000 × *g* at 4°C or at room temperature. To solubilize the actin cytoskeleton, Triton-insoluble fractions were resuspended in Triton buffer with 1 M KI (1, 32) and kept for 15 min on ice. Protein was precipitated from the supernatant with acetone.

Expression of GST fusion proteins and GST pull-down analysis. GST fusion proteins of human importin α and importin β or GST alone were expressed in *Escherichia coli* and purified using glutathione-Sepharose (Amersham). HeLa cells were lysed with Triton buffer on ice, and the lysates were incubated for 2 h at 4°C with GST or GST fusion proteins coupled to glutathione-Sepharose. Bound proteins were pelleted by centrifugation, washed three times in Triton buffer, and processed for SDS-polyacrylamide gel electrophoresis and Western blotting.

Heterokaryon assay. HeLa cells were transfected with vectors coding for EGFP-fusion proteins, excess transfection reagent was removed, and cells were cocultured with NIH 3T3 fibroblasts. Cycloheximide (75 μg/ml; 30 min) was added to halt protein expression, and cell bodies were fused with 50% polyethylenglycole 8000 in DMEM for 2 min. Cells were maintained for 2 h in DMEM containing 50 μg/ml cycloheximide in the absence or presence of 20 nM leptomycin B (LMB) and fixed with 4% paraformaldehyde and permeabilized with 0.1% Triton in PBS. After incubation in blocking solution (5% bovine serum albumin in PBST), cells were stained with DAPI (1 μg/ml) and rhodamine-phalloidine (0.4 U/ml each).

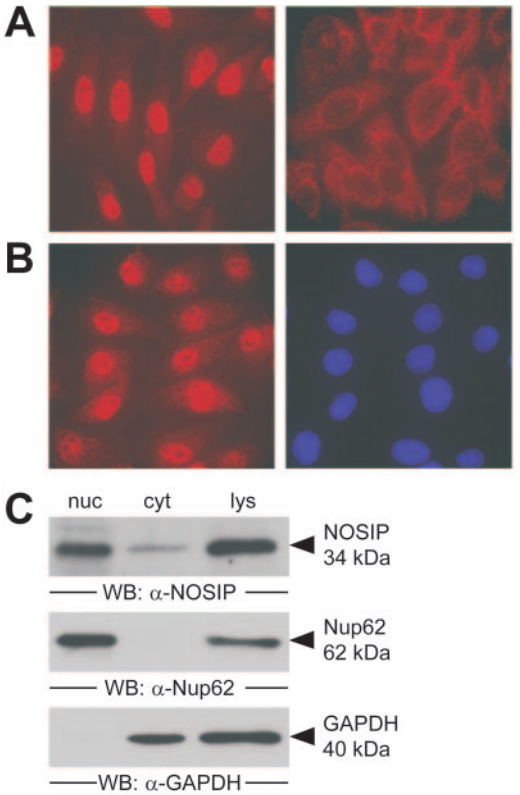

FIG. 1. NOSIP resides preferentially in the nuclei of cultured cells. Subcellular distribution of endogenous NOSIP analyzed by indirect immunofluorescence microscopy in EA.hy296 (A) and HeLa (B) cells and subcellular fractionation of HeLa cells, followed by Western blotting of equalized sample volumes with anti-NOSIP (C). DNA is counterstained with DAPI (B, right). Nuclear (nuc) and cytoplasmic (cyt) fractions are identified by marker proteins Nup62 and GAPDH (C). WB, Western blotting; lys, lysate.

Arginine-citrulline conversion assay. CHO-NOS or EA.hy926 cells were incubated at 37°C for 30 min in HEPES buffer (20 mM HEPES-Na, pH 7.4, containing 150 mM NaCl, 5 mM KCl, 1 mM $MgSO_4$, 1 mM $CaCl_2$, 10 μM L-arginine, 0.2 mg/ml glucose). Cells were stimulated with the calcium ionophore A23187 (3 μM) for 15 min in the presence of 3.3 μCi/ml L-[^{14}C]arginine. To follow the conversion to L-[^{14}C]citrulline (27), cells were denatured with cold ethanol, and soluble cellular components were dissolved in 20 mM HEPES-Na, pH 5.5, and applied to 2-ml columns of Dowex AG50WX-8 (Na^+ form). The radioactivity in the eluate containing L-[^{14}C]citrulline was quantified by liquid scintillation counting. Unless otherwise indicated, NOS-specific L-[^{14}C]citrulline production was calculated as the difference of the respective radioactivity count to the value of cells pretreated with 100 μM of NOS inhibitor L-N^G-nitro-L-arginine.

RESULTS

NOSIP is localized preferentially in the nuclei of cultured cells. Initially we analyzed the subcellular distribution of endogenous NOSIP in the endothelium-derived cell line EA.hy926. In accordance with the previously observed localization in situ (20), we observed a differential distribution pattern for NOSIP in cultured cells, where the vast majority of cells showed preferential nuclear NOSIP localization (Fig. 1A, left); in rare subpopulations, however, we observed a depletion of the nucleus and enrichment of NOSIP in the cytoplasm (Fig. 1A, right). This dual distribution pattern, which we demon-

strated here for EA.hy926 cells, was also observed in C2C12, CHO, COS, HeLa, human umbilical vein endothelial, and NIH 3T3 cells (data not shown). To employ an appropriate cell line to study protein shuttling, we analyzed the relative levels of endogenous nuclear versus cytoplasmic NOSIP in HeLa cells, revealing that NOSIP was primarily targeted to the nucleus and that only a small fraction was present in the cytoplasm (Fig. 1B and C).

NOSIP nuclear localization is mediated by a bipartite NLS binding to importin α. Sequence analysis of human NOSIP did not reveal a canonical mono- or bipartite NLS, corresponding to the consensus sequences which mediate interaction with transport proteins of the import family (5, 16). Rather NOSIP displays a sequence segment rich in basic amino acid residues between positions 78 and 101 (Fig. 2A), which could serve as the NLS. To test this hypothesis, we analyzed the subcellular distribution of wild-type (wt) NOSIP and various NOSIP mutants by subcellular fractionation and indirect immunofluorescence microscopy (Fig. 2B and C). Both methods revealed that wt NOSIP accumulates in the nucleus of transfected cells. In contrast, mutant NOSIP, where the complete putative NLS had been deleted, was conspicuously absent from the nuclear fraction (Fig. 2B, ΔNLS) and showed predominant cytoplasmic staining in indirect immunofluorescence microscopy (Fig. 2C). Deletion of the major C-terminal basic cluster (ΔC2) and mutation of the minor N-terminal cluster (m2A) (Fig. 2B and C) attenuated nuclear accumulation of NOSIP, indicating that they are both necessary for efficient nuclear import. Thus, NOSIP appears to have a bipartite NLS consisting of two basic clusters separated by a spacer of 10 residues. Furthermore, we were able to demonstrate that the NLS of NOSIP is sufficient to mediate nuclear import of heterologous proteins up to 80 kDa, confirming that the NLS per se is functional (data not shown). Hereafter, we refer to the sequence between positions 78 and 101 as NOSIP-NLS.

The default mechanism for nuclear import comprises recognition of the cargo NLS by importin α, which then in turn binds importin β, targeting the trimeric complex to the nuclear pore (3). Therefore, we studied the binding of NOSIP and NLS mutants thereof to importin α by GST pull-down assays. Recombinantly expressed and purified GST-importin α precipitated endogenous NOSIP (data not shown) and wt NOSIP from lysates of transiently transfected HeLa cells, whereas the construct pulled down only a minor fraction of m2A and failed to pull-down ΔNLS and ΔC2 (Fig. 2D). These data demonstrate that NOSIP nuclear import is mediated by binding of NOSIP to the importin complex via its NLS.

NOSIP shuttles between nucleus and cytoplasm. To address the question of whether cytoplasmic localization of NOSIP is a consequence of export from the nucleus, we analyzed the nucleocytoplasmic shuttling of NOSIP in a heterokaryon assay. This was carried out in the absence and presence of LMB, an inhibitor of CRM1-dependent export. To this end HeLa cells were transfected with EGFP fusion proteins and fused with NIH 3T3 fibroblasts, and shuttling between nuclei within the fused cell body was analyzed. Nucleocytoplasmic shuttling of the NOSIP-EGFP fusion protein was detected both in the absence (data not shown) and in the presence of LMB (Fig. 3A and B). In contrast, the control cargo p53-EGFP underwent nucleocytoplasmic shuttling only in the absence of LMB (data not shown) and was retained by HeLa nuclei in the presence of LMB (Fig. 3C and D). These results indicate that NOSIP is exported from the nucleus and shuttles constantly between nucleus and cytoplasm in an LMB-dependent manner.

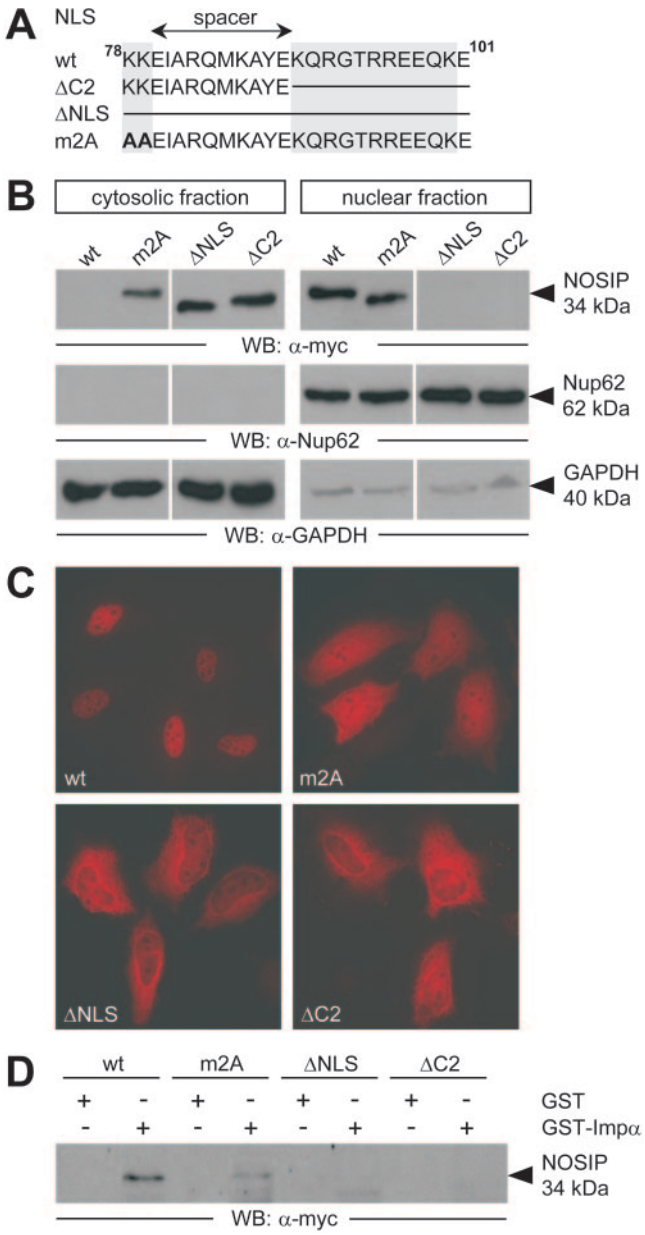

FIG. 2. Nuclear import of NOSIP is mediated by a bipartite NLS binding to importin α. Between positions 78 and 101, human NOSIP exhibits two basic clusters (gray boxes) separated by a spacer of 10 residues (A). HeLa cells were transiently transfected with N-terminally myc-tagged wt-NOSIP (wt), with deletion mutants of NOSIP, where the complete sequence (ΔNLS, positions 78 to 101) or the C-terminal basic cluster (ΔC2, positions 90 to 101) have been deleted, and with a point mutant, where basic residues in the N-terminal cluster have been mutated to alanine (m2A). Subcellular distribution was analyzed by subcellular fractionation, followed by Western blotting (B) or indirect immunofluorescence microscopy (C). Lysates of transiently transfected HeLa cells were utilized for GST pull-down analysis with GST-importin α (GST-Impα) or GST. Recombinant proteins were detected using anti-myc (B, C, and D).

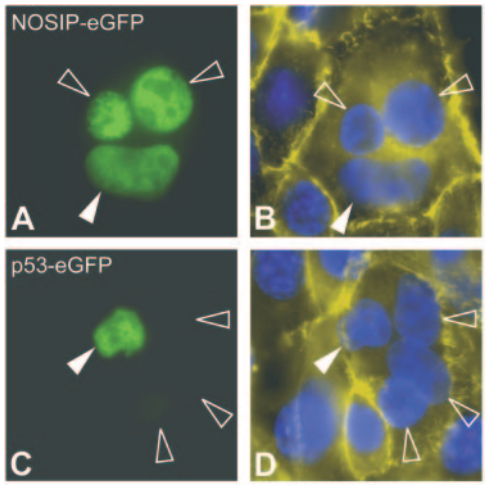

FIG. 3. NOSIP is a nucleocytoplasmic shuttling protein. The shuttling ability of NOSIP-EGFP was tested by the heterokaryon assay (A). Cell borders are visualized by rhodamine-phalloidin staining. DAPI staining allows discrimination between murine NIH 3T3 (open arrowheads) and HeLa nuclei (filled arrowheads) (B and D). Inhibition of nucleocytoplasmic shuttling of p53-eGFP in the presence of leptomycin B served as negative control (C).

Cytoplasmic NOSIP translocates eNOS to the cytoskeleton and inhibits eNOS activity. We have previously reported that pronounced overexpression of NOSIP results in its cytoplasmic accumulation and drives translocation of eNOS from the plasma membrane to Triton-insoluble intracellular compartments (6), suggesting that extranuclear localization of NOSIP may be essential for eNOS trafficking. Therefore, we tested the capacity of NLS-deficient NOSIP mutants to induce eNOS translocation in CHO-NOS cells from the Triton-soluble to the Triton-insoluble cell fraction, with the presence of the latter being commonly attributed to association with the cytoskeleton. All NOSIP mutants showed an unimpaired capacity to interact with eNOS as demonstrated by coimmunoprecipitation (data not shown). Overexpression of NLS-deficient NOSIP mutants caused a significant shift of eNOS from the Triton-soluble to the Triton-insoluble cell fraction (designated fraction 1) compared to wt NOSIP- or mock-transfected cells (Fig. 4A). Addition of the F-actin depolymerizing agent, potassium iodide (1, 32), to the Triton-insoluble fraction (yielding fraction 2) led to a complete solubilization of eNOS (Fig. 4B), strongly arguing for an association of eNOS with the actin cytoskeleton. To demonstrate that eNOS was not associated with lipid rafts in the Triton-insoluble fraction 1, we did the preparation at room temperature throughout, i.e., under conditions where lipid-rich domains are known to be solubilized (1), and found that this treatment did not promote solubilization of eNOS (Fig. 4C). Likewise, application of cytochalasin D, blocking actin polymerization in intact cells, completely blunted NOSIP-induced translocation of eNOS to the Triton-insoluble fraction 1 (Fig. 4D). These results demonstrate that NOSIP has the capacity to translocate eNOS to the Triton-insoluble fraction, the putative actin cytoskeleton, and that cytoplasmic localization of NOSIP is mandatory to induce redistribution of eNOS. We have previously reported that eNOS translocation was accompanied by reduction of NO production

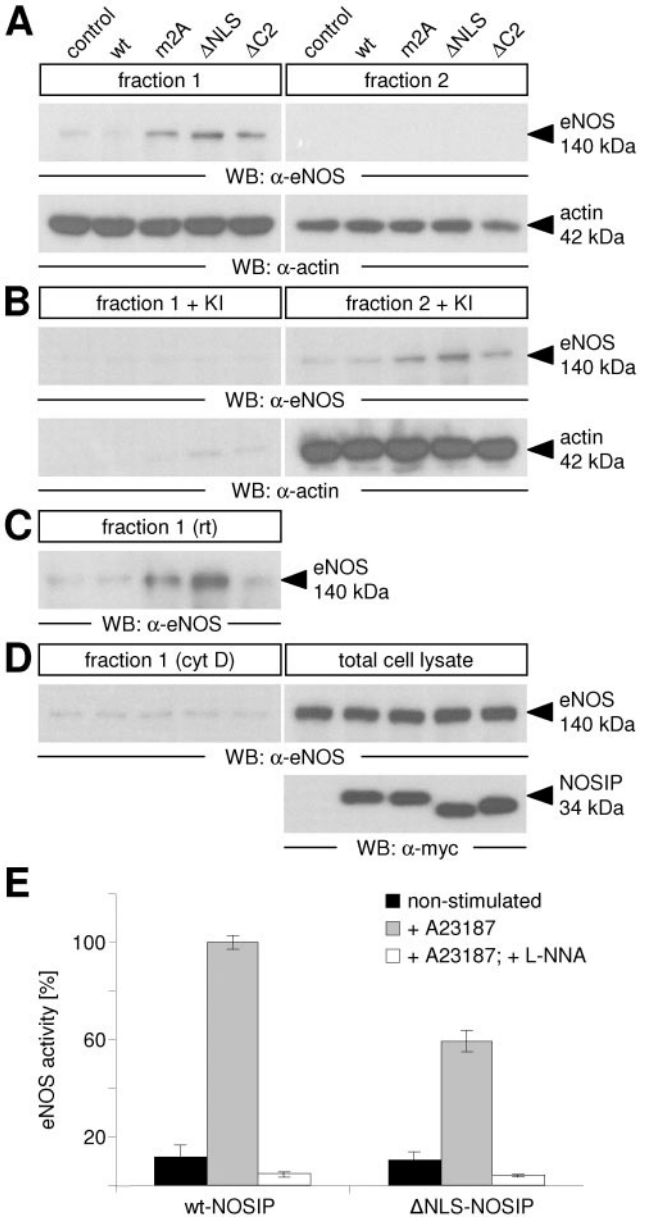

FIG. 4. Cytoplasmic NOSIP translocates eNOS to the actin cytoskeleton and inhibits its activity. CHO-NOS cells transiently transfected with myc-tagged wt NOSIP, m2A, ΔNLS, or ΔC2 were used to prepare Triton-insoluble cytoskeletal fractions (fraction 1) at 4°C (A) or at room temperature (rt; C), and presence of eNOS and actin was probed by anti-eNOS and anti-actin, respectively. Actin was solubilized from fraction 1 by adding 1 M KI in Triton buffer, and the presence of eNOS and actin was assayed in the resultant soluble fraction (fraction 2) (B). Alternatively, actin polymerization was inhibited by preincubation with 1 μM cytochalasin D (cyt D) prior to fractionation (D). Total eNOS levels were identical throughout and equivalent amounts of the various NOSIP mutants were expressed (D). A23187-stimulated eNOS activity in CHO-NOS cells transfected with wt or ΔNLS was measured by the arginine-citrulline conversion assay in the absence and presence of NOS inhibitor L-N^G-nitro-L-arginine (E). WB, Western blotting.

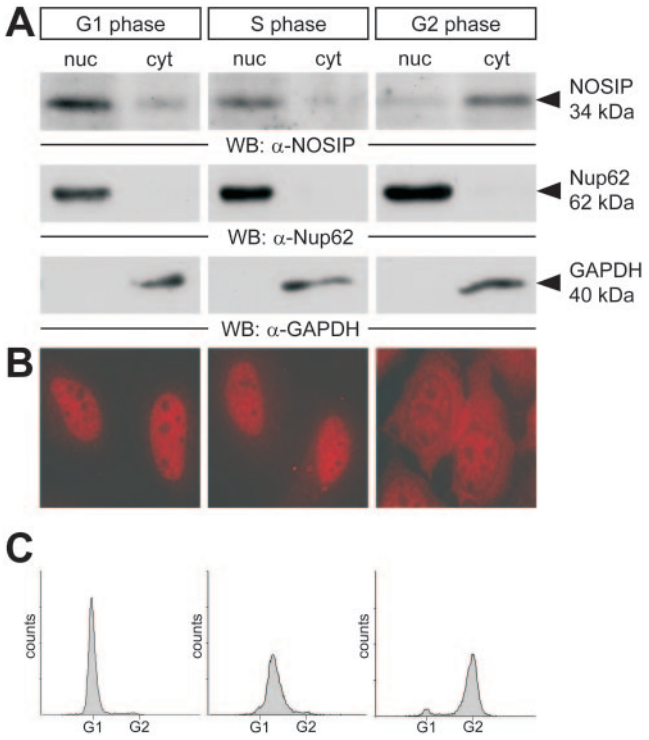

FIG. 5. NOSIP translocates to the cytoplasm in the G_2 phase of the cell cycle. Distribution of endogenous NOSIP in synchronized HeLa cells during different phases of the cell cycle was analyzed by subcellular fractionation (A) and indirect immunofluorescence (B) using anti-NOSIP. Cytoplasmic (cyt) and nuclear (nuc) fractions were stained for marker proteins as detailed in the legend of Fig. 1. Synchronization was monitored by FACS analysis (C). WB, Western blotting.

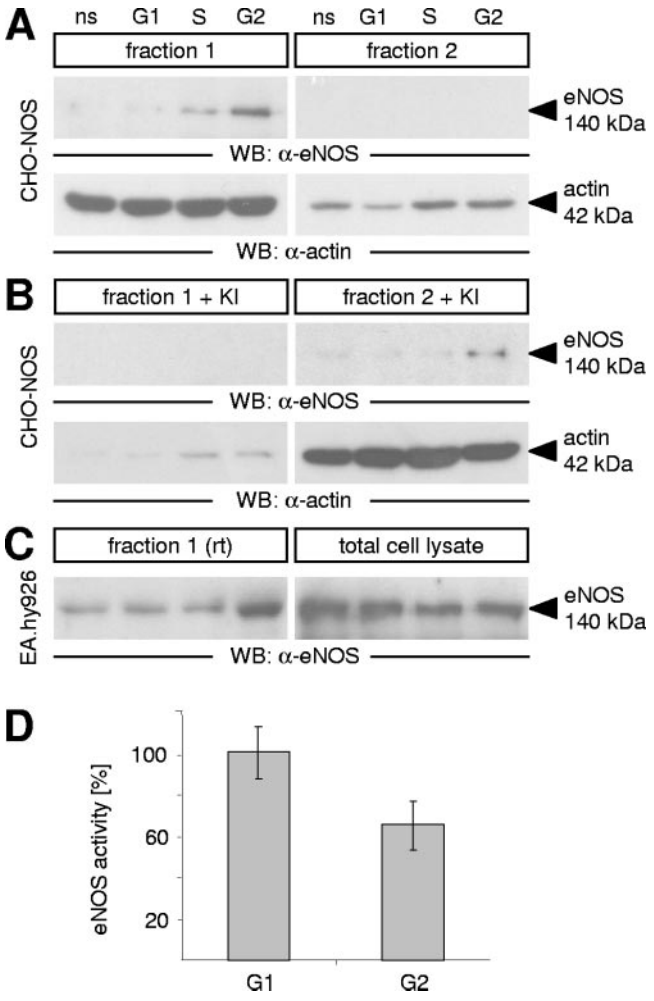

FIG. 6. eNOS is targeted to the cytoskeleton and eNOS activity is inhibited in G_2. Presence of eNOS in the Triton-insoluble fraction 1 of synchronized CHO-NOS cells was tested during different phases of the cell cycle using anti-eNOS (A). Triton-insoluble fraction 1 was incubated with KI in Triton buffer to depolymerize actin, and the presence of eNOS was assayed in the resultant soluble fraction 2 (B). Triton-insoluble fraction 1 prepared from synchronized EA.hy926 cells at room temperature (rt) was tested for the presence of eNOS (C). A23187-stimulated eNOS activity in EA.hy926 cells in G_1 and G_2 was measured by the arginine-citrulline conversion assay (D). Synchronization was monitored by FACS analysis (not shown). WB, Western blotting; ns, nonsynchronized.

(6). Therefore, we tested whether overexpression of the constitutively cytoplasmic NOSIP ΔNLS mutant had an effect on eNOS activity. Indeed, the cytoskeletal association of eNOS induced by overexpression of ΔNLS was paralleled by a 40% reduction of A23187-induced activity (Fig. 4E), indicating that the cytoplasmic localization of NOSIP is necessary and sufficient to mediate eNOS trafficking and inhibition.

NOSIP translocates to the cytoplasm in the G_2 phase of the cell cycle. Since many nucleocytoplasmic shuttling proteins belong to the group of cell cycle-associated proteins (11), we investigated the subcellular distribution pattern of NOSIP in HeLa cells in relation to cell cycle progression. Synchronization into G_2 yielded 4.84% of cells in G_1, 23.58% in S, and 71.58% in G_2 phase (Fig. 5C). In the G_1 and S phases of the cell cycle, NOSIP was predominantly nuclear. In marked contrast, cells in G_2 accumulated NOSIP in their cytoplasm, while nuclear NOSIP levels were reduced (Fig. 5). This translocation occurred clearly before disassembly of the nuclear membrane prior to mitosis. Analysis of the cell cycle-specific distribution of NOSIP in CHO-NOS and EA.hy926 cells gave similar results (data not shown). We conclude that the subcellular localization of NOSIP is subject to dynamic regulation and that nuclear NOSIP is translocated to the cytoplasm in the G_2 phase of the cell cycle.

NOSIP induces cytoskeletal targeting of eNOS in G_2 and reduces eNOS activity. Given the effects of cytoplasmic NOSIP on eNOS translocation and activity, one may ask whether cytoplasmic accumulation of endogenous NOSIP in G_2 is paralleled by a shift of eNOS to the cytoskeletal fraction and enzymatic inhibition. In asynchronous CHO-NOS cells, a minute fraction (2.3%) of the total cellular eNOS pool is associated with the cytoskeleton, while the vast majority of eNOS (>97%) is associated with the Triton-soluble fraction (data not shown). In CHO-NOS cells synchronized into G_2, the fraction of Triton-insoluble eNOS increased sharply (Fig. 6A) by a factor of 10.3, accounting for approximately 24% of the total eNOS amount (not shown). This effect was reversed by the addition of KI (Fig. 6B) and persisted upon preparation at room temperature (data not shown), strongly arguing for a cell cycle-specific association of eNOS with the actin cytoskeleton in G_2.

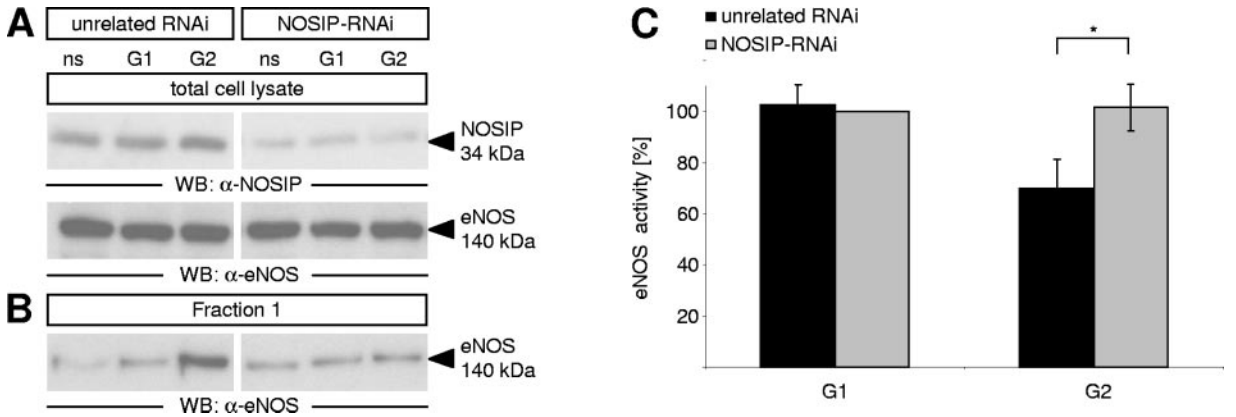

FIG. 7. NOSIP knockdown abolishes cytoskeletal association and inhibition of eNOS in G_2. Following transient transfection of CHO-NOS cells with unrelated or NOSIP-specific RNAi vectors and subsequent synchronization, NOSIP and eNOS levels in cell lysates were analyzed by Western blotting with anti-NOSIP and anti-eNOS (A). Association of eNOS with the cytoskeletal fraction was determined as detailed in the legend of Fig. 6 (B), and synchronization was monitored by FACS (not shown). A23187-stimulated eNOS activity was measured by the arginine-citrulline conversion assay (C). WB, Western blotting; ns, nonsynchronized.

Furthermore, we employed the endothelium-derived cell line EA.hy926 endogenously expressing eNOS and NOSIP and observed a similar G_2-specific association of eNOS with the cytoskeleton (Fig. 6C), demonstrating the functionality of this regulatory mechanism in a physiologically relevant cell system. Analysis of the enzymatic capacity of eNOS during cell cycle progression of EA.hy926 cells revealed that the A23187-induced eNOS activity dropped significantly by 35% in G_2 (Fig. 6D). Thus, it appears that eNOS is targeted to the cytoskeleton in G_2 and that eNOS residing in the cytoskeletal compartment may not be activated in response to $[Ca^{2+}]_i$ transients.

NOSIP knockdown impairs redistribution of eNOS and restores full enzymatic capacity in G_2. To test whether reduction of eNOS activity in G_2 is indeed mediated by NOSIP, we probed for the consequences of RNAi-mediated silencing of NOSIP on eNOS solubility and activity in G_1 and G_2. Compared to CHO-NOS cells transiently transfected with a vector expressing unrelated RNAi, a vector targeting NOSIP mRNA significantly reduced NOSIP protein levels, while expression of eNOS remained unchanged (Fig. 7A). Under these conditions, cells transfected with unrelated RNAi showed cytoskeletal association of eNOS (Fig. 7B) and reduction of eNOS activity in G_2 by 24% (Fig. 7C), whereas the knockdown of NOSIP following transfection with NOSIP-RNAi prevented G_2-specific translocation and inhibition of eNOS (Fig. 7B and C). Apparently, the degree of inhibition reflects the amount of eNOS associated with the cytoskeleton under these conditions. Together our results indicate that eNOS is specifically inhibited in the G_2 phase of the cell cycle due to targeting to the actin cytoskeleton, and this regulatory mechanism critically depends on the presence of NOSIP.

DISCUSSION

The biological importance of extensive eNOS regulation is stressed by the fact that temporal control of activity is complemented by spatial control of local availability through vectorial targeting of eNOS to distinct subcellular compartments (15). As yet, the molecular underpinnings of the intracellular trafficking processes are largely unknown. In the present study we describe a novel aspect of regulation of eNOS localization and activity in respect to the cell cycle and assign a precise function to its interacting protein, NOSIP, in targeting eNOS to the cytoskeleton and modulating its activity in a cell cycle-dependent manner.

NOSIP undergoes constitutive nuclear import and export, albeit at different rates, and the relative efficiency dictates NOSIP localization. We envisage that in most cell cycle phases import outbalances export, resulting in predominant nuclear localization of NOSIP, while in G_2 the balance is shifted toward export. However, the exact mechanism remains to be determined. Nuclear import is facilitated through the binding of NOSIP to importin α, which is dependent on the integrity of its NLS. The NLS of NOSIP does not exactly fit the consensus sequence $KRX_{10-12}KRXK$ (5) in that basic amino acids are more widely spread over the C-terminal cluster; however, the identification of a functional nonconsensus NLS (9, 29) indicates that some degree of sequence variability is well tolerated by the nuclear import machinery. Nuclear export of NOSIP is not inhibited by the CRM1-specific export inhibitor LMB, a property NOSIP shares, e.g., with RelA (19) and hepatitis delta virus surface protein HDAg-L (22), and this observation is well reflected by the fact that NOSIP lacks a typical leucine-rich export signal. Whether NOSIP is exported in a truly CRM1-independent process or whether it utilizes an LMB-insensitive binding site of CRM1, as recently shown for $p27^{kip}$ (4), remains to be determined. As shown for the tyrosine kinase c-Abl (35), regulated nucleocytoplasmic shuttling might provide a mechanism for rapid alteration of subcellular distribution to "switch" between distinct nuclear and cytosolic functions (35). Alternatively, nucleocytoplasmic shuttling could function to transmit signals from the nucleus into the cytoplasm or vice versa, as in the case of Smad1, where nuclear export allows for ligand-induced coupling with cell surface receptors (38).

Though we can clearly assign a function to cytoplasmic NOSIP in the regulation of eNOS localization and activity, we can only speculate about the distinct nuclear function(s) of

NOSIP. Controversial reports describe nuclear localization of eNOS, e.g., under pathological conditions (14), but firm experimental evidence under physiological conditions is still lacking. Though NOSIP could clearly represent a prime candidate for a nuclear shuttle protein for eNOS, we have no experimental data to date in support of this notion. Given the moderate frequency of extranuclear NOSIP localization in situ (7, 8, 20, 21), it is very possible that stimuli other than cell cycle progression might also drive the nuclear export of NOSIP. For example, we have been able to induce nuclear export of NOSIP in primary hippocampal neurons by application of *N*-methyl-D-aspartate/glycine (8). In the same study we demonstrated the interaction of NOSIP with neuronal NOS and characterized their functional relationship in the nervous system, pointing to a common role of NOSIP in the control of localization and activity of both eNOS and neuronal NOS.

Based on the data presented here, we propose that NOSIP exerts its inhibitory effect on eNOS by interfering with its association with "active" compartments such as the plasma membrane and targeting it to the cytoskeleton. This is congruent with our previous finding that binding of NOSIP to eNOS per se does not adversely affect the activity of the enzyme, but NOSIP and the caveolin scaffolding domain compete for interaction with eNOS, strongly suggesting that NOSIP interferes with caveolar association of eNOS (6). Moreover, this notion is well reflected by the independent findings that cochaperone CHIP interacts with the eNOS/hsp90 complex, causing eNOS to redistribute to an inactive detergent-insoluble compartment, presumably cytoskeleton, and that $CHIP^{-/-}$ cells exhibit elevated eNOS activity. Of note, the trafficking process mediated by CHIP is independent of its ubiquitin ligase activity (18). Ubiquitin ligase activity has also been demonstrated for NOSIP (10); however, the potential involvement of this activity in cell cycle-dependent partitioning of eNOS remains to be defined.

It was recently suggested that the cytoskeleton plays a more decisive role in the regulation of eNOS activity than previously thought (34, 39). Indeed, eNOS has been shown to interact directly with actin, and stabilization of actin filaments with phalloidin enhances the association of eNOS with F-actin and at the same time impairs eNOS activity (33). On the other hand, some reports describe the association of active eNOS with Triton-insoluble compartments, the putative actin cytoskeleton (2). Also, eNOS was found to translocate to intercellular junctions in response to cell-cell contact formation, an event associated with increased activity and enrichment of eNOS in the Triton-insoluble fraction (13). To what extent the direct interaction between eNOS and actin contribute to eNOS activity control remains to be established. With the findings described herein, however, we provide conclusive evidence that eNOS association with the cytoskeleton in G_2 leads to inhibition, since loss of eNOS activity in the G_2 phase appears to be directly correlated with the amount of eNOS bound to the cytoskeleton. In view of the distinct distribution of eNOS among various cellular compartments, translocation of 35% of the eNOS pool to the cytoskeleton as observed in EA.hy926 cells may well reflect complete depletion of the enzyme from, e.g., the active plasmalemmal compartment. It should be noted that we observed elevated specific basal eNOS activity in EA.hy926 cells synchronized by a double thymidine block in comparison to unsynchronized cells, which we currently cannot account for. We have also made efforts to extend our studies to primary endothelial cells, where 10% of the eNOS pool is associated with the Triton-insoluble fraction even in the asynchronous state (12); however, the lack of desired reproducibility in the synchronization of primary endothelial cells prevented their use for cell cycle studies.

In the vascular system NO is believed to maintain an antiproliferative environment in the vessel wall (30). The antiproliferative effect of NO is thought to be mediated mainly by up-regulation of p53 gene expression (25), induction of expression and inhibition of degradation of cell cycle inhibitor $p21^{cip/waf}$ (23, 25), and/or negative regulation of the levels of cyclin A and its associated kinase (23). Moreover, the addition of exogenous NO has been reported to cause cell cycle arrest in G_2 (17, 26, 31, 36). Thus, delicate regulation of endogenous NO biosynthesis through the cell cycle appears to be critical for tight control of the cell proliferation and apoptosis machinery, e.g., during embryonic development, vascular remodeling and angiogenesis in wound healing, tumor vascularization, and postischemia. Moreover, one might speculate that attenuation of the enzymatic capacity of eNOS prior to disassembly of the nuclear envelope might help protect the DNA from the toxic effects of NO (24). In conclusion, we find eNOS activity altered within the cell cycle through targeted compartmentation, which is critically dependent on the nucleocytoplasmic shuttling of NOSIP. These findings define a molecular basis for cell cycle-dependent alterations of endogenous NO production that is critical for the well-documented downstream effects of NO, e.g., in apoptosis and cell proliferation.

ACKNOWLEDGMENTS

We thank Günter Blobel and Tarik Soliman (Rockefeller University, New York, NY) for the generous gift of karyopherin cDNAs, Hans Clevers and Marc van de Wetering (Hubrecht Laboratory, Utrecht, The Netherlands) for the $pTER^{+}$ vector, Ludger Hengst (Max Planck Institute, Munich, Germany) for the heterokaryon protocol, Sabine Graf (University of Frankfurt) for excellent technical assistance, and Daniela Höller and the Institute for Biochemistry II members for constructive criticism and helpful discussions.

This work was supported by a grant of the Deutsche Forschungsgemeinschaft through the Sonderforschungsbereich 553 (B3).

REFERENCES

1. **Brown, D. A., and J. K. Rose.** 1992. Sorting of GPI-anchored proteins to glycolipid-enriched membrane subdomains during transport to the apical cell surface. Cell **68:**533–544.
2. **Chatterjee, S., S. Cao, T. E. Peterson, R. D. Simari, and V. Shah.** 2003. Inhibition of GTP-dependent vesicle trafficking impairs internalization of plasmalemmal eNOS and cellular nitric oxide production. J. Cell Sci. **116:** 3645–3655.
3. **Chook, Y. M., and G. Blobel.** 2001. Karyopherins and nuclear import. Curr. Opin. Struct. Biol. **11:**703–715.
4. **Connor, M. K., R. Kotchetkov, S. Cariou, A. Resch, R. Lupetti, R. G. Beniston, F. Melchior, L. Hengst, and J. M. Slingerland.** 2003. CRM1/Ran-mediated nuclear export of p27(Kip1) involves a nuclear export signal and links p27 export and proteolysis. Mol. Biol. Cell **14:**201–213.
5. **Conti, E., and E. Izaurralde.** 2001. Nucleocytoplasmic transport enters the atomic age. Curr. Opin. Cell Biol. **13:**310–319.
6. **Dedio, J., P. Konig, P. Wohlfart, C. Schroeder, W. Kummer, and W. Muller-Esterl.** 2001. NOSIP, a novel modulator of endothelial nitric oxide synthase activity. FASEB J. **15:**79–89.
7. **Dreyer, J., D. Hirlinger, W. Muller-Esterl, S. Oess, and R. Kuner.** 2003. Spinal upregulation of the nitric oxide synthase-interacting protein NOSIP in a rat model of inflammatory pain. Neurosci. Lett. **350:**13–16.
8. **Dreyer, J., M. Schleicher, A. Tappe, K. Schilling, T. Kuner, G. Kusumawidijaja, W. Muller-Esterl, S. Oess, and R. Kuner.** 2004. Nitric oxide synthase (NOS)-interacting protein interacts with neuronal NOS and regulates its distribution and activity. J. Neurosci. **24:**10454–10465.

9. **Ems-McClung, S. C., Y. Zheng, and C. E. Walczak.** 2004. Importin alpha/beta and Ran-GTP regulate XCTK2 microtubule binding through a bipartite nuclear localization signal. Mol. Biol. Cell **15:**46–57.
10. **Friedman, A. D., D. Nimbalkar, and F. W. Quelle.** 2003. Erythropoietin receptors associate with a ubiquitin ligase, p33RUL, and require its activity for erythropoietin-induced proliferation. J. Biol. Chem. **278:**26851–26861.
11. **Gama-Carvalho, M., and M. Carmo-Fonseca.** 2001. The rules and roles of nucleocytoplasmic shuttling proteins. FEBS Lett. **498:**157–163.
12. **Garcia-Cardena, G., P. Oh, J. Liu, J. E. Schnitzer, and W. C. Sessa.** 1996. Targeting of nitric oxide synthase to endothelial cell caveolae via palmitoylation: implications for nitric oxide signaling. Proc. Natl. Acad. Sci. USA **93:**6448–6453.
13. **Govers, R., L. Bevers, P. de Bree, and T. J. Rabelink.** 2002. Endothelial nitric oxide synthase activity is linked to its presence at cell-cell contacts. Biochem. J. **361:**193–201.
14. **Govers, R., and S. Oess.** 2004. To NO or not to NO: "where?" is the question. Histol. Histopathol. **19:**585–605.
15. **Govers, R., and T. J. Rabelink.** 2001. Cellular regulation of endothelial nitric oxide synthase. Am. J. Physiol. Renal Physiol. **280:**F193–F206.
16. **Hodel, M. R., A. H. Corbett, and A. E. Hodel.** 2001. Dissection of a nuclear localization signal. J. Biol. Chem. **276:**1317–1325.
17. **Janssen, Y. M., R. Soultanakis, K. Steece, E. Heerdt, R. J. Singh, J. Joseph, and B. Kalyanaraman.** 1998. Depletion of nitric oxide causes cell cycle alterations, apoptosis, and oxidative stress in pulmonary cells. Am. J. Physiol. **275:**L1100–L1109.
18. **Jiang, J., D. Cyr, R. W. Babbitt, W. C. Sessa, and C. Patterson.** 2003. Chaperone-dependent regulation of endothelial nitric-oxide synthase intracellular trafficking by the co-chaperone/ubiquitin ligase CHIP. J. Biol. Chem. **278:**49332–49341.
19. **Kelly, D., J. I. Campbell, T. P. King, G. Grant, E. A. Jansson, A. G. Coutts, S. Pettersson, and S. Conway.** 2004. Commensal anaerobic gut bacteria attenuate inflammation by regulating nuclear-cytoplasmic shuttling of PPAR-gamma and RelA. Nat. Immunol. **5:**104–112.
20. **Konig, P., J. Dedio, W. Muller-Esterl, and W. Kummer.** 2002. Distribution of the novel eNOS-interacting protein NOSIP in the liver, pancreas, and gastrointestinal tract of the rat. Gastroenterology **123:**314–324.
21. **Konig, P., J. Dedio, S. Oess, T. Papadakis, A. Fischer, W. Muller-Esterl, and W. Kummer.** 2005. NOSIP and its interacting protein, eNOS, in the rat trachea and lung. J. Histochem. Cytochem. **53:**155–164.
22. **Lee, C. H., S. C. Chang, C. H. Wu, and M. F. Chang.** 2001. A novel chromosome region maintenance 1-independent nuclear export signal of the large form of hepatitis delta antigen that is required for the viral assembly. J. Biol. Chem. **276:**8142–8148.
23. **Maejima, Y., S. Adachi, H. Ito, K. Nobori, M. Tamamori-Adachi, and M. Isobe.** 2003. Nitric oxide inhibits ischemia/reperfusion-induced myocardial apoptosis by modulating cyclin A-associated kinase activity. Cardiovasc. Res. **59:**308–320.
24. **Marnett, L. J., J. N. Riggins, and J. D. West.** 2003. Endogenous generation of reactive oxidants and electrophiles and their reactions with DNA and protein. J. Clin. Investig. **111:**583–593.
25. **Mizuno, S., M. Kadowaki, Y. Demura, S. Ameshima, I. Miyamori, and T. Ishizaki.** 2004. p42/44 Mitogen-activated protein kinase regulated by p53 and nitric oxide in human pulmonary arterial smooth muscle cells. Am. J. Respir. Cell Mol. Biol. **31:**184–192.
26. **Mohr, S., T. S. McCormick, and E. G. Lapetina.** 1998. Macrophages resistant to endogenously generated nitric oxide-mediated apoptosis are hypersensitive to exogenously added nitric oxide donors: dichotomous apoptotic response independent of caspase 3 and reversal by the mitogen-activated protein kinase kinase (MEK) inhibitor PD 098059. Proc. Natl. Acad. Sci. USA **95:**5045–5050.
27. **Nuszkowski, A., R. Grabner, G. Marsche, A. Unbehaun, E. Malle, and R. Heller.** 2001. Hypochlorite-modified low density lipoprotein inhibits nitric oxide synthesis in endothelial cells via an intracellular dislocalization of endothelial nitric-oxide synthase. J. Biol. Chem. **276:**14212–14221.
28. **Richardson, R. T., I. N. Batova, E. E. Widgren, L. X. Zheng, M. Whitfield, W. F. Marzluff, and M. G. O'Rand.** 2000. Characterization of the histone H1-binding protein, NASP, as a cell cycle-regulated somatic protein. J. Biol. Chem. **275:**30378–30386.
29. **Sekimoto, T., M. Fukumoto, and Y. Yoneda.** 2004. 14-3-3 suppresses the nuclear localization of threonine 157-phosphorylated p27(Kip1). EMBO J. **23:**1934–1942.
30. **Sessa, W. C.** 2004. eNOS at a glance. J. Cell Sci. **117:**2427–2429.
31. **Shao, C., Y. Furusawa, and M. Aoki.** 2003. Sper/NO-induced reversible proliferation inhibition and cycle arrests associated with a micronucleus induction in HSG cells. Nitric Oxide **8:**83–88.
32. **Stickney, J. T., W. C. Bacon, M. Rojas, N. Ratner, and W. Ip.** 2004. Activation of the tumor suppressor merlin modulates its interaction with lipid rafts. Cancer Res. **64:**2717–2724.
33. **Su, Y., S. Edwards-Bennett, M. R. Bubb, and E. R. Block.** 2003. Regulation of endothelial nitric oxide synthase by the actin cytoskeleton. Am. J. Physiol. Cell Physiol. **284:**C1542–C1549.
34. **Su, Y., S. I. Zharikov, and E. R. Block.** 2002. Microtubule-active agents modify nitric oxide production in pulmonary artery endothelial cells. Am. J. Physiol. Lung Cell Mol. Physiol. **282:**L1183–L1189.
35. **Taagepera, S., D. McDonald, J. E. Loeb, L. L. Whitaker, A. K. McElroy, J. Y. Wang, and T. J. Hope.** 1998. Nuclear-cytoplasmic shuttling of C-ABL tyrosine kinase. Proc. Natl. Acad. Sci. USA **95:**7457–7462.
36. **Takagi, K., Y. Isobe, K. Yasukawa, E. Okouchi, and Y. Suketa.** 1994. Nitric oxide blocks the cell cycle of mouse macrophage-like cells in the early G2+M phase. FEBS Lett. **340:**159–162.
37. **van de Wetering, M., I. Oving, V. Muncan, M. T. Pon Fong, H. Brantjes, D. van Leenen, F. C. Holstege, T. R. Brummelkamp, R. Agami, and H. Clevers.** 2003. Specific inhibition of gene expression using a stably integrated, inducible small-interfering RNA vector. EMBO Rep. **4:**609–615.
38. **Xiao, Z., A. M. Brownawell, I. G. Macara, and H. F. Lodish.** 2003. A novel nuclear export signal in Smad1 is essential for its signaling activity. J. Biol. Chem. **278:**34245–34252.
39. **Zharikov, S. I., A. A. Sigova, S. Chen, M. R. Bubb, and E. R. Block.** 2001. Cytoskeletal regulation of the L-arginine/NO pathway in pulmonary artery endothelial cells. Am. J. Physiol. Lung Cell Mol. Physiol. **280:**L465–L473.
40. **Zimmermann, K., N. Opitz, J. Dedio, C. Renne, W. Muller-Esterl, and S. Oess.** 2002. NOSTRIN: a protein modulating nitric oxide release and subcellular distribution of endothelial nitric oxide synthase. Proc. Natl. Acad. Sci. USA **99:**17167–17172.